Article

Influence of Backbone Conformations of Human Carbonic Anhydrase II on Carbon Dioxide Hydration: Hydration Pathways and Binding of Bicarbonate

Markus J. Loferer, Christofer S. Tautermann, Hannes H. Loeffler, and Klaus R. Liedl

J. Am. Chem. Soc., **2003**, 125 (29), 8921-8927• DOI: 10.1021/ja035072f • Publication Date (Web): 25 June 2003

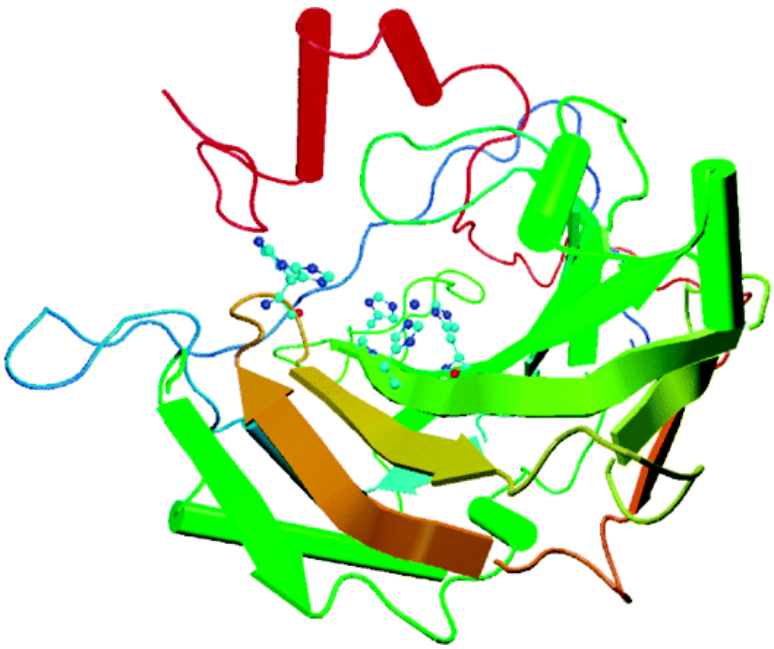

J|A|C|S
ARTICLES
Published on Web 06/25/2003

Influence of Backbone Conformations of Human Carbonic Anhydrase II on Carbon Dioxide Hydration: Hydration Pathways and Binding of Bicarbonate

Markus J. Loferer, Christofer S. Tautermann, Hannes H. Loeffler, and Klaus R. Liedl*

Contribution from the Institute of General, Inorganic and Theoretical Chemistry, University of Innsbruck, Innrain 52a, A-6020 Innsbruck, Austria

Received March 10, 2003; E-mail: klaus.liedl@uibk.ac.at

Abstract: In this study, the hydration of carbon dioxide and the formation of bicarbonate in human carbonic anhydrase II have been examined. From semiempirical QM/MM molecular dynamics studies, dominant conformations of the protein backbone, possibly contributing to the catalytic activity, have been isolated and further examined by means of density functional QM/MM methods. In agreement with experimental observations, a binding site for cyanate, which acts as an inhibitor, has been located, whereas for carbon dioxide, depending on the conformation of the protein environment, either a different binding site or no binding site has been found. In the latter case, carbon dioxide diffuses barrierless to the zinc-bound oxygen, and then a weakly bound bicarbonate complex is formed. The formed complex is characterized by a long C−O bond to the zinc-bound hydroxide. The nature of the calculated stationary points was verified by determination of vibrational frequencies. Finally, the dissociation of the formed bicarbonate from zinc has been considered. Therefore, a water molecule was included in the QM zone of the QM/MM hybrid potential, and minimization yielded a pentacoordinated intermediate. From a potential energy scan, an activation energy of 6.2 kcal/mol for dissociation of bicarbonate from Zn has been found.

Introduction

Carbonic anhydrase is a ubiquitous enzyme which has been found in all animals and photosynthesizing organisms[1,2] examined for its presence to date. One essential physiological function is to catalyze the hydration of carbon dioxide and the back-reaction, the dehydration of bicarbonate.[3−6] The human carbonic anhydrase family consists of seven distinct isozymes,[1] of which carbonic anhydrase II (HCA II) is the most thoroughly studied form. It is characterized by an exceptionally high carbon dioxide turnover rate of 10^6 s^{-1} at pH 9 and 25 °C.[7−10] Several high-resolution X-ray structures[11−18] have revealed the active site of carbonic anhydrase, which − although not strictly conserved among all isozymes[19−21] − works similarly and contains a catalytically required zinc ion.[22] It is coordinated by three histidine residues (HIS94, HIS96, and HIS119)[23−25] and by a fourth ligand which is a water molecule or a hydroxide depending on the pH. Several other residues are essential for catalysis,[26−28] as has been verified by site-specific mutagenesis:[29] THR199 and THR200 interact directly[30,31] with the zinc-bound species, and together with GLU106 and active site water

(1) Lindskog, S. *Pharmacol. Ther.* **1997**, *74*, 1−20.
(2) Smith, K. S.; Jakubzick, C.; Whittam, T. S.; Ferry, J. G. *Proc. Natl. Acad. Sci. U.S.A.* **1999**, *96*, 15184−15189.
(3) Simonsson, I.; Jonsson, B. H.; Lindskog, S. *Eur. J. Biochem.* **1979**, *93*, 409−417.
(4) Silverman, D. N.; Lindskog, S. *Acc. Chem. Res.* **1988**, *21*, 30−36.
(5) Lipscomb, W. N. *Annu. Rev. Biochem.* **1983**, *52*, 17−34.
(6) Liang, J.-Y.; Lipscomb, W. N. *Biochemistry* **1988**, *27*, 8676−8683.
(7) Silverman, D. N.; Lindskog, S.; Tu, C. K.; Wynns, G. C. *J. Am. Chem. Soc.* **1979**, *101*, 6734−6740.
(8) Rowlett, R. S.; Silverman, D. N. *J. Am. Chem. Soc.* **1982**, *104*, 6737−6747.
(9) Silverman, D. N. *Methods Enzymol.* **1995**, *249*, 479−503.
(10) Zhang, X.; Hubbard, C. D.; van Eldik, R. *J. Phys. Chem.* **1996**, *100*, 9161−9171.
(11) Liljas, A.; Kannan, K. K.; Bergstein, P.-C.; Waara, I.; Fridborg, K.; Strandberg, B.; Carlbom, U.; Jörup, L.; Lövgren, S.; Petev, M. *Nature, New Biol.* **1972**, *235*, 131−137.
(12) Kannan, K. K.; Notstrand, B.; Fridborg, K.; Lövgren, S.; Ohlsson, A.; Petef, M. *Proc. Natl. Acad. Sci. U.S.A.* **1975**, *72*, 51−55.
(13) Kannan, K. K.; Petef, M.; Fridborg, K.; Cid-Dresdner, H.; Lövgren, S. *FEBS Lett.* **1977**, *73*, 115−119.
(14) Eriksson, A. E.; Jones, T. A.; Liljas, A. *Proteins: Struct., Funct., Genet.* **1988**, *4*, 274−282.
(15) Eriksson, A. E.; Kylsten, P. M.; Jones, T. A.; Liljas, A. *Proteins: Struct., Funct., Genet.* **1988**, *4*, 283−293.
(16) Hakansson, K.; Carlsson, M.; Svensson, L. A.; Liljas, A. *J. Mol. Biol.* **1992**, *227*, 1192−1204.
(17) Nair, S. K.; Christanson, D. W. *Eur. J. Biochem.* **1993**, *213*, 507−515.
(18) Xue, Y.; Vidgren, J.; Svensson, L. A.; Liljas, A.; Jonsson, B.-H.; Lindskog, S. *Proteins* **1993**, *15*, 80−87.
(19) Tashian, R. E. *Adv. Genet.* **1993**, *30*, 321−356.
(20) Tripp, B. C.; Smith, K.; Ferry, J. G. *J. Biol. Chem.* **2001**, *276*, 48615−48618.
(21) Liljas, A.; Laurberg, M. *EMBO Rep.* **2000**, *1*, 16−17.
(22) Christianson, D. W.; Cox, J. D. *Annu. Rev. Biochem.* **1999**, *68*, 33−57.
(23) Kiefer, L. L.; Ippolito, J. A.; Fierke, C. A.; Christianson, D. W. *J. Am. Chem. Soc.* **1993**, *115*, 12581−12582.
(24) Kiefer, L. L.; Paterno, S. A.; Fierke, C. A. *J. Am. Chem. Soc.* **1995**, *117*, 6831−6837.
(25) Christianson, D. W.; Fierke, C. A. *Acc. Chem. Res.* **1996**, *29*, 331−339.
(26) Merz, K. M., Jr. *J. Mol. Biol.* **1990**, *214*, 799−802.
(27) Lesburg, C. A.; Christianson, D. W. *J. Am. Chem. Soc.* **1995**, *117*, 6838−6844.
(28) Huang, S.; Sjöblom, B.; Sauer-Eriksson, A. E.; Jonsson, B.-H. *Biochemistry* **2002**, *41*, 7628−7635.
(29) Liang, Z.; Xue, Y.; Behravan, G.; Jonsson, B.-H.; Lindskog, S. *Eur. J. Biochem.* **1993**, *211*, 821−827.
(30) Krebs, J. F.; Ippolito, J. A.; Christianson, D. W.; Fierke, C. A. *J. Biol. Chem.* **1993**, *268*, 27458−27466.
(31) Merz, K. M., Jr.; Banci, L. *J. Am. Chem. Soc.* **1997**, *119*, 863−871.

molecules they form a hydrogen bonding network which extends toward bulk water. The putative role of this hydrogen bonding network is proton transfer from the zinc-bound species to HIS64,[32−35] located at the entrance of the active site cavity. At least two intervening water molecules are necessary[32,33] to bridge the transfer distance of 7.5 Å. The mechanism of this proton-transfer step, which is the rate-determining step at high buffer concentrations, is the subject of active research.[36−40]

In the most widely accepted catalytic mechanism[4,9,41−44] for the enzymatic activity of HCA II, the deprotonation of zinc-bound water constitutes the first of three catalytic steps.[45] The second step − which this study is mainly focusing on − is the hydration of carbon dioxide leading to the formation of a zinc-bound bicarbonate. In a subsequent step, the bicarbonate is substituted by active site water, and the catalytic cycle is closed. Additionally, proton-transfer steps[4,5,46] in the bound bicarbonate might be required for efficient dissociation of the product.

Several key factors influencing the efficiency of the hydration step of carbon dioxide have been elucidated in past years: The zinc hydroxide−THR199−GLU106 hydrogen bonding network forces the hydroxide oxygen atom to present a lone electron pair to the incoming carbon dioxide[26] and thus enables rapid formation of the product. The exact location and binding of carbon dioxide has not yet been detected and is still a controversial issue. On the basis of theoretical studies, Merz et al. propose two binding sites[47] with the closer site 3.0 Å away from the zinc-bound hydroxide, and a molecular dynamics study of Liang et al.[48] predicts a similar result. From X-ray structures of inhibitor complexes,[16,49] a binding site, 3.4 Å away from the zinc, has been proposed, which is formed by the side chains of VAL121, VAL143, LEU198, and TRP209. Interaction with the protein is assumed to lead to an electrophilic activation of the carbon dioxide for the subsequent nucleophilic attack of the zinc-bound hydroxide. A part of the binding energy of the in situ formed carboxylate in this hydrophobic cavity might then be utilized to lower the activation energy for dissociation of the product.[16]

A great impetus in the detailed understanding of the catalysis of carbonic anhydrase has come from the study of model systems, and, although none of them can compete in catalytic activity with the native enzyme, many structural and mechanistic properties of carbonic anhydrase have been revealed by the aid of these complexes.[50−52]

Likewise, computational chemistry has been used to investigate carbonic anhydrase for a long while. Beginning with the seminal paper of Liang and Lipscomb,[53] which studied the hydration of carbon dioxide in the gas phase, many helpful contributions have come from theoretical studies.[31,38,39,54−64] However, the study of enzymatic reactions still remains a challenge in the field of computational chemistry, because of the size of the enzymes and the distinguished influence of a heterogeneous molecular environment on the course of a reaction. As ab initio and density functional methods in hybrid QM/MM potentials are now available,[65] it is possible to simulate enzymatic reactions in their natural environment to a good degree of quantitative accuracy at an affordable cost.

Here, a QM/MM study of the hydration of carbon dioxide in HCA II is presented. All calculations have been performed in a consistent manner with density functional methods for the QM-part of the QM/MM hybrid potential. The determination of stationary points and corresponding energies of important steps leading to the formation of bicarbonate was the goal of this study.

Computational Methods

As the starting structure, the 1.54 Å resolution X-ray structure of human carbonic anhydrase II complexed with bicarbonate[16] was used and retrieved from the Brookhaven Protein Data Bank[66] (PDB ID: 2CBA). The protonation state of titratable side chains was determined by continuum electrostatics methods,[67] and the remaining charge of +2 was neutralized by the addition of two counterions. Charges for carbon dioxide and for zinc-bound hydroxide were determined by an ESP method as implemented in Gaussian 98[68] for the initial setup and minimization of the enzyme. For all other residues, standard parameters

(32) Steiner, H.; Jonsson, B.-H.; Lindskog, S. *Eur. J. Biochem.* **1975**, *59*, 253−259.
(33) Tu, C. K.; Silverman, D. N.; Forsman, C.; Jonsson, B.-H.; Lindskog, S. *Biochemistry* **1989**, *28*, 7913−7918.
(34) Jackman, J. E.; Merz, K. M., Jr.; Fierke, C. A. *Biochemistry* **1996**, *35*, 16421−16428.
(35) Qian, M.; Tu, C.; Earnhardt, J. N.; Laipis, P. J.; Silverman, D. N. *Biochemistry* **1997**, *36*, 15758−15764.
(36) Lu, D.; Voth, G. A. *J. Am. Chem. Soc.* **1998**, *120*, 4006−4014.
(37) Pomes, R.; Roux, B. *Biophys. J.* **1998**, *75*, 33−40.
(38) Isaev, A.; Scheiner, S. *J. Phys. Chem. B* **2001**, *105*, 6420−6426.
(39) Nemukhin, A. V.; Topol, I. A.; Grigorenko, B. L.; Burt, S. K. *J. Phys. Chem. B* **2002**, *106*, 1734−1740.
(40) Nakata, K.; Shimomura, N.; Shiina, N.; Izumi, M.; Ichikawa, K.; Shiro, M. *J. Inorg. Biochem.* **2002**, *89*, 255−266.
(41) Bertini, I.; Luchinat, C. *Acc. Chem. Res.* **1983**, *16*, 272−279.
(42) Lindskog, S.; Liljas, A. *Curr. Opin. Struct. Biol.* **1993**, *3*, 915−920.
(43) Liljas, A.; Hakansson, K.; Jonsson, B. H.; Xue, Y. *Eur. J. Biochem.* **1994**, *219*, 1−10.
(44) Northrop, D. B.; Simpson, F. B. *Arch. Biochem. Biophys.* **1998**, *353*, 288−292.
(45) Jonsson, B. H.; Steiner, H.; Lindskog, S. *FEBS Lett.* **1976**, *64*, 310−314.
(46) Liang, J.-Y.; Lipscomb, W. N. *Biochemistry* **1987**, *26*, 5293−5301.
(47) Merz, K. M., Jr. *J. Am. Chem. Soc.* **1991**, *113*, 406−411.
(48) Liang, J. Y.; Lipscomb, W. N. *Proc. Natl. Acad. Sci. U.S.A.* **1990**, *87*, 3675−3679.
(49) Lindahl, M.; Svensson, L. A.; Liljas, A. *Proteins: Struct., Funct., Genet.* **1993**, *15*, 177−182.
(50) Zhang, X.; van Eldik, R. *Inorg. Chem.* **1995**, *34*, 5606−5614.
(51) Mao, Z.-W.; Liehr, G.; van Eldik, R. *J. Chem. Soc., Dalton Trans.* **2001**, 1593−1600.
(52) Kimura, E. *Acc. Chem. Res.* **2001**, *34*, 171−179.
(53) Liang, J. Y.; Lipscomb, W. N. *J. Am. Chem. Soc.* **1986**, *108*, 5051−5058.
(54) Toba, S.; Colombo, G.; Merz, K. M., Jr. *J. Am. Chem. Soc.* **1999**, *121*, 2290−2302.
(55) Mauksch, M.; Bräuer, M.; Weston, J.; Anders, E. *ChemBioChem* **2001**, *2*, 190−198.
(56) Muguruma, C. *J. Mol. Struct.* (*THEOCHEM*) **1999**, *461−462*, 439−452.
(57) Hartmann, M.; Merz, K. M., Jr.; van Eldik, R.; Clark, T. *J. Mol. Model.* **1998**, *4*, 355−365.
(58) Nguyen, M. T.; Ha, T.-K. *J. Am. Chem. Soc.* **1984**, *106*, 599−602.
(59) Isaev, A. N. *J. Mol. Struct. (THEOCHEM)* **2002**, *582*, 195−203.
(60) Suarez, D.; Merz, K. M., Jr. *J. Am. Chem. Soc.* **2001**, *123*, 3759−3770.
(61) Garmer, D. R. *J. Phys. Chem. B* **1997**, *101*, 2945−2953.
(62) Bräuer, M.; Perez-Lustres, J. L.; Weston, J.; Anders, E. *Inorg. Chem.* **2002**, *41*, 1454−1463.
(63) Merz, K. M., Jr.; Banci, L. *J. Phys. Chem.* **1996**, *100*, 17414−17420.
(64) Sinnecker, S.; Bräuer, M.; Koch, W.; Anders, E. *Inorg. Chem.* **2001**, *40*, 1006−1013.
(65) Lyne, P. D.; Hodoscek, M.; Karplus, M. *J. Phys. Chem. A* **1999**, *103*, 3462−3471.
(66) Berman, H. M.; Westbrook, J.; Feng, Z.; Gilliland, G.; Bhat, T. N.; Weissig, H.; Shindyalov, I. N.; Bourne, P. E. *Nucleic Acids Res.* **2000**, *28*, 235−242.
(67) Schaefer, M.; Sommer, M.; Karplus, M. *J. Phys. Chem. B* **1997**, *101*, 1663−1683.
(68) Frisch, M. J.; Trucks, G. W.; Schlegel, H. B.; Scuseria, G. E.; Robb, M. A.; Cheeseman, J. R.; Zakrzewski, V. G.; Montgomery, J. J. A.; S., E.; Burant, J. C.; Dapprich, S.; Millam, J. M.; Daniels, A. D.; Kudin, K. N.; Strain, M. C.; Farkas, O.; Tomasi, J.; Barone, V.; Cossi, M.; Cammi, R.; Mennucci, B.; Pomelli, C.; Adamo, C.; Clifford, S.; Ochterski, J.; Petersson, G. A.; Ayala, P. Y.; Cui, Q.; Morokuma, K.; Malick, D. K.; Rabuck, A. D.; Raghavachari, K.; Foresman, J. B.; Cioslowski, J.; Ortiz, J. V.; Stefanov, B. B.; Liu, G.; Liashenko, A.; Piskorz, P.; Komaromi, I.; Gomperts, R.; Martin, R. L.; Fox, D. J.; Keith, T.; Al-Laham, M. A.; Peng, C. Y.; Nanayakkara, A.; Gonzales, C.; Challacombe, M.; Gill, P. M. W.; Johnson, B.; Chen, W.; Wong, M. W.; Andres, J. L.; Gonzales, C.; Head-Gordon, M.; Replogle, E. S.; Pople, J. A. *Gaussian 98*, revision A.5; Gaussian, Inc.: Pittsburgh, PA, 1998.

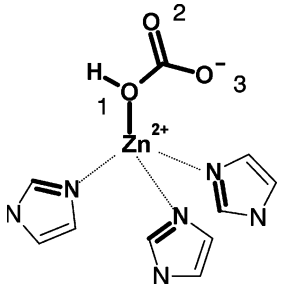

Figure 1. Overview of the reactive center and numbering scheme. The subsystem which is computed by quantum mechanical methods is drawn in bold. The quantum mechanically treated part of the histidines had to be complemented by two link atoms which are not shown here.

were used.[69] Apart from the crystal waters, 121 TIP3P water molecules were added in a 16 Å sphere around the reactive center by a series of minimizations and high-temperature MD runs until no more water molecules could be added.

Throughout this work, all considered systems were studied by means of QM/MM methods.[70] Density functional theory at the level of B3LYP associated with a 6-31G(d) or 6-31+G(d,p) basis set was employed for geometry optimizations; for single-point energies of selected stationary points, enlarged basis sets (6-311++G(d,p), 6-311G(d,p) for the zinc atom) were used. All calculations were performed with GAMESS-US,[71] which was interfaced with CHARMM[72] version c28b2.

QM/MM boundaries were handled with link atoms which cut across single bonds. Each link atom was treated as a proper QM atom and thus exposed to the field of all surrounding point charges. Following other QM/MM studies, the link atom was forced by bond and angle restraints to maintain geometry.[73] The charge of the bordering MM atom was set to zero and redistributed to other atoms of the adjacent group to maintain electroneutrality. Here, the zinc atom and the hydrogen carbonate were part of the QM zone. To keep the computational efforts in a practicable range, the three zinc-coordinating imidazole rings were split into a QM area and a MM area, such that a methylenamine analogue was treated by ab initio methods and the interface was along (formal) single bonds. Field et al. advise against cutting across conjugated bonds,[70] and the authors are aware that such a partition is not desirable as a general case; however, the histidines here are only indirectly involved in catalysis. Initial tests also resulted in geometries comparable to those of systems where the entire histidine side chains have been incorporated in the QM zone. In all calculations, the distance $Zn-N_{His}$ remained in a range of 2.0−2.2 Å, that is, in the range of the experimentally found distances. A graphical representation of the QM/MM setup can be found in Figure 1.

All minimizations included the QM region and all MM atoms in a 12-Å sphere around the geometrical center of the QM region. The atoms outside of this region were kept fixed for all geometries after an initial minimization. Stationary points were verified by the calculation of numerical second derivatives. Because of the large number of energy and gradient evaluations, it was necessary to restrict the number of atoms comprised in the calculation of second derivatives to those contained in the QM zone. All other atoms were kept fixed during this calculation. Also, all pseudoatoms were excluded from the evaluation.

Results and Discussion

Simulation Results. Molecular dynamics studies are a valuable tool for exploring the conformational space and for overcoming local minima. Thus, we have employed CHARMM together with the PM3 semiempirical Hamiltonian to simulate HCA II. Semiempirical methods have already been successfully applied to this enzyme.[31,63] Although these methods are in most cases not appropriate to model transition states because of their limitation to the built-in parameters, geometries for local minima are generally of good quality. Thus, we decided to explore the conformational space by means of semiempirical QM/MM molecular dynamics; the found − dominant − conformations were then used as input to QM/MM calculations employing density functional methods to provide high-quality geometries and energies. Two models were studied in the simulations: bicarbonate with the hydroxide bound to zinc (O1, see Figure 1) and bicarbonate with a carboxylate oxygen (O2, Figure 1) coordinated to the zinc.

For both models, 50 ps of simulation was performed. The QM section comprised the three zinc-coordinating histidines, zinc, hydroxide, and carbon dioxide. Standard simulation protocols were employed including a Langevin setup, stochastic boundary conditions, and a time step of 0.5 fs. The prevalent conformations for the bound bicarbonate are essentially those of the studies of Merz et al.[31] However, alterations from the starting structure occurred in the protein backbone. Specifically, and most important for the following examinations, as the residues involved are closely located to the active site, the torsional angle Ψ_{199}, that is, the backbone dihedral formed by THR199−N, THR199−CA, THR199−C, and THR200−N, twists to a mean of −34° from the initial 0° (Figure 2), and the peptide NH of THR200 thus partially points into the presumed carbon dioxide binding cavity. The standard deviations for both simulations are 12° and 15°, respectively, which indicates structural flexibility such that a continuum of conformations in an interval spanned by a dihedral angle of about −10° to −50° might be significantly populated in vivo. Thus, several of the following calculations were made using both the minimized starting structure, corresponding to the X-ray structure with a dihedral angle of approximately 0° (structure I), and the (minimized) resulting structure from the QM/MM molecular dynamics runs with a dihedral angle of approximately −30° (structure II).

The Binding of Carbon Dioxide. The first set of QM/MM minimizations addressed the location of a binding site for carbon dioxide. Hitherto, no binding site for carbon dioxide has been detected by crystallographic methods. Cyanate which acts as an inhibitor, however, has been found[49] to bind in a site formed by the amino acid residues VAL121, VAL143, LEU198, and TRP209. The bound cyanate is 3.4 Å away from the zinc ion and hydrogen bonds to the NH group of THR199. Thus, as a starting point for QM/MM calculations, a carbon dioxide was placed to the position where cyanate has been found. In parallel to this calculation and for reference purposes, a minimization with the cyanate was also done. The outcome of both calculations was completely different: Whereas cyanate remains tightly

(69) MacKerell, A. D.; Bashford, D.; Bellott, M.; Dunbrack, R. L.; Evanseck, J. D.; Field, M. J.; Fischer, S.; Gao, J.; Guo, H.; Ha, S.; Joseph-McCarthy, D.; Kuchnir, L.; Kuczera, K.; Lau, F. T. K.; Mattos, C.; Michnick, S.; Ngo, T.; Nguyen, D. T.; Prodhom, B.; Reiher, W. E., III; Roux, B.; Schlenkrich, M.; Smith, J. C.; Stote, R.; Straub, J.; Watanabe, M.; Wiorkiewicz-Kuczera, J.; Yin, D.; Karplus, M. *J. Phys. Chem. B* **1998**, *102*, 3586−3616.
(70) Field, M. J.; Bash, P. A.; Karplus, M. *J. Comput. Chem.* **1990**, *11*, 700−733.
(71) Schmidt, M. W.; Baldridge, K. K.; Boatz, J. A.; Elbert, S. T.; Gordon, M. S.; Jensen, J. H.; Koseki, S.; Matsunaga, N.; Nguyen, K. A.; Su, S. J.; Windus, T. L.; Dupuis, M.; Montgomery, J. A. *J. Comput. Chem.* **1993**, *14*, 1347−1363.
(72) Brooks, B. R.; Bruccoleri, R. E.; Olafson, B. D.; States, D. J.; Swaminathan, S.; Karplus, M. *J. Comput. Chem.* **1983**, *4*, 187−217.
(73) Reuter, N.; Dejaegere, A.; Maigret, B.; Karplus, M. *J. Phys. Chem. A* **2000**, *104*, 1720−1735.

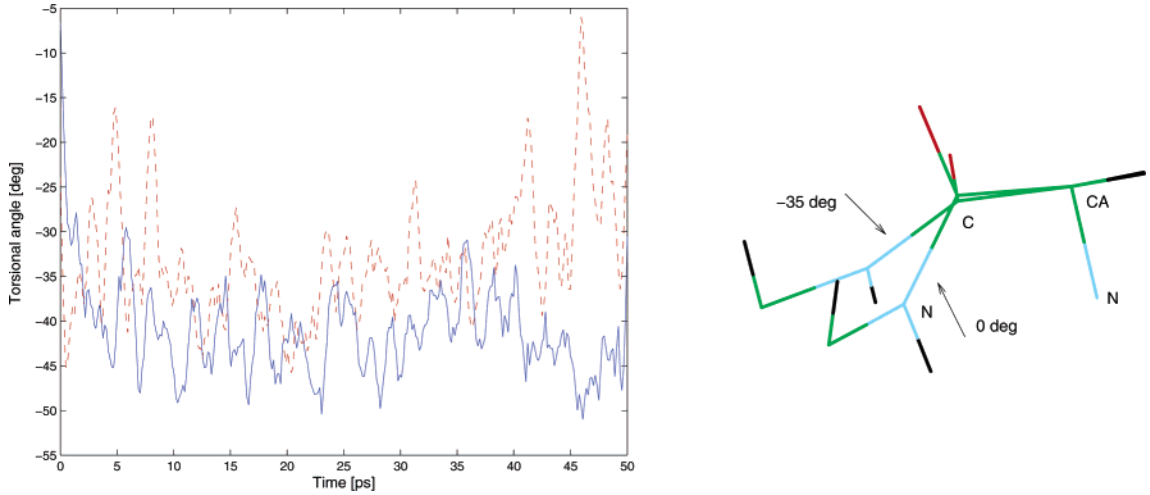

Figure 2. Left: The torsional angles for Ψ_{199} are drawn for the two semiempirical QM/MM simulations performed. The dashed line shows the result for the simulation where bicarbonate binds with the hydroxy group to zinc; the solid line shows the result for the simulation where bicarbonate binds with a carboxy oxygen to zinc. The average dihedral angle of both simulations is −35.3° (solid line, −37.4°; dashed line, −33.1°); however, significant fluctuations occur. Right: A typical backbone conformation found in the simulation with $\Psi_{199} = -35°$ (termed "structure II" in the text) and the starting conformation (0°) which corresponds to the X-ray structure ("structure I").

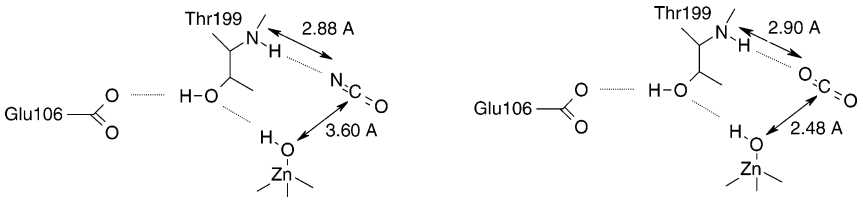

Figure 3. Structural arrangement of bound cyanate (left) and bound carbon dioxide (right). The binding mode of carbon dioxide is similar to that of cyanate with a hydrogen bond to the peptide NH of THR199, but it is placed closer to the zinc-bound hydroxide as compared to cyanate.

bound in the binding site, carbon dioxide diffuses toward the zinc-bound hydroxide for both of the examined structures I and II.

Cyanate belongs to a group of inhibitors which act as metal poison but do not replace or interact with the zinc-bound solvent. From the X-ray structure of Lindahl et al.,[49] it is evident that cyanate is tightly bound to the N−H of THR199 with its negatively charged nitrogen terminus, thus acting as an inhibitor. The results of the QM/MM minimizations are in good agreement with this. The binding mode is the same with the oxygen terminus of cyanate forming bonds with the solvent and the hydroxyl group of THR200 and the nitrogen terminus pointing toward N−H of THR199. The carbon of cyanate is 3.6 Å away from the oxygen of zinc-bound hydroxide (Figure 3, left).

This result corroborates the studies with carbon dioxide bound instead of cyanate: For both structures I and II, carbon dioxide was placed to the binding site of cyanate and subsequently minimized. For the X-ray structure I, optimization resulted in a geometry where carbon dioxide is bound closer to zinc with a distance of 2.48 Å between the carbon of carbon dioxide and the zinc-bound oxygen (Figure 3, right), but the tight interaction with NH of THR199 found for cyanate persists. In structure II, carbon dioxide diffuses directly toward the reactive center and forms bicarbonate. To overcome artificial unfavorable interactions which could force the carbon dioxide away from the initial binding site of cyanate, the minimizations were repeated with constraints forcing carbon dioxide to distances of 2.5, 3.0, and 3.5 Å away from the zinc-bound hydroxide. However, after relaxation of these constraints, carbon dioxide moved either toward the catalytic center (structure II) or to the position 2.48 Å away from the oxygen (structure I). The geometry of structure II, where carbon dioxide was restrained to a distance of 2.50 Å away, shows the carbon dioxide rotated about an angle of 90° to the peptide N−H of THR199, displaying a hydrogen bond to that and a weaker one to N−H of THR200 (3.36 Å heavy atom distance). This interaction most likely forces the reorientation of carbon dioxide and thus impedes binding to this site. Additionally, potential energy scans were performed for both structures I and II. The distance from the carbon of carbon dioxide to the zinc-bound oxygen was for each case constrained to a series of fixed values, and all other degrees of freedom were minimized. The corresponding potential energy surface can be found in Figure 4. Structure I (top) exhibits a minimum located around 2.5 Å, which is easily recognized as the found binding site. The other energy minimum is located at 1.65 Å and corresponds to a very weakly bonded bicarbonate. This will be discussed in detail below. For structure II (Figure 4, bottom), no energy minima have been found consistent with the findings mentioned above.

Atom charges and bond orders can be found in Table 1. The highly positively charged carbon (+0.63) for the bound carbon dioxide (termed "intermediate" in Table 1) is remarkable as it is significantly more positive than the carbon of in vacuo carbon dioxide and also surmounts the values for the bound products. Thus, the increase of electrophilicity by the protein environment is probably a main contributor to the catalytic efficiency of HCA II.

Although an interaction of bound carbon dioxide via a hydrogen bond to THR199 has already been suggested,[47,48] our observations do not fully comply with the outcome of molecular

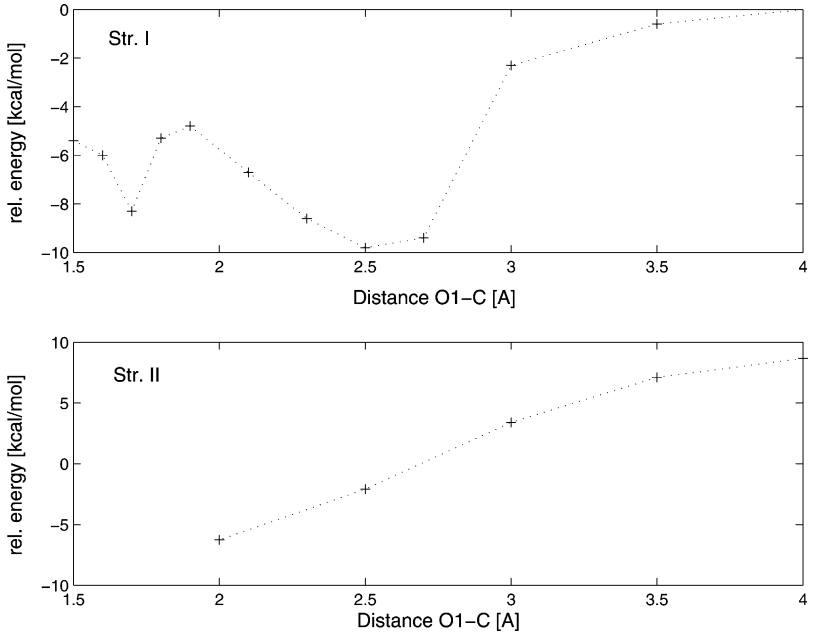

Figure 4. Results of energy scans along the distance O1−C. Top: The energy scan of structure I shows a minimum located around 2.5 Å which corresponds to the binding of carbon dioxide. Another minimum at 1.7 Å can be assigned to the product geometry. Bottom: Carbon dioxide diffuses barrierless toward the reactive site. The energies refer to the total potential energy of structure I with a O1−C distance of 4.0 Å which has been set to 0. All energies have been evaluated employing the B3LYP hybrid density functional and a 6-31G(d) basis set for the QM part of the QM/MM potential.

Table 1. Atom Charges and Bond Orders for the Intermediate and the Found Product Minima[a]

	atom charge					bond order			
system	Zn	O1	C	O2	O3	Zn–O1	C–O1	C–O2	C–O3
intermediate	0.14	−0.70	+0.63	−0.34	−0.33	1.07	<0.05	1.87	1.89
min I	−0.01	−0.35	+0.41	−0.55	−0.40	0.85	0.51	1.72	1.93
min II	0.58	−0.35	+0.38	−0.57	−0.46	0.73	0.63	1.76	1.85
CO_2 vacuum			+0.31	−0.16	−0.16			1.99	2.01

[a] Gas-phase values of carbon dioxide have also been included for comparison. The carbon in the intermediate structure is highly positively charged and thus a strong electrophile. Mulliken charges have been assigned from a single-point energy calculation, employing a 6-311++G(d,p) basis set for the QM region.

dynamics studies of these authors, which find a binding site for carbon dioxide located 3−4 Å from the zinc ion, which is essentially the above-mentioned binding pocket for cyanate. The experimental evidence that cyanate binding and carbon dioxide hydration energy do not change in parallel as the side chain of residue VAL143 is made increasingly large[74,75] might indicate a different binding mode for both and can thus be interpreted in support of our observation.

Structures of Bound Bicarbonate. As mentioned above, minimization of the geometry of structure I gave a zinc-bound bicarbonate as the result of a nucleophilic attack of the zinc-bound hydroxide oxygen on the carbon. The same structure was obtained by a QM/MM minimization of structure II, when carbon dioxide was placed close enough to the zinc-bound hydroxide to overcome the energy barrier at around 2.0 Å. To ameliorate the quality of the minimized structures, the employed basis set for the QM part of the QM/MM potential was enlarged by the addition of polarization functions to all hydrogen atoms and of diffuse functions to all heavy atoms except zinc.

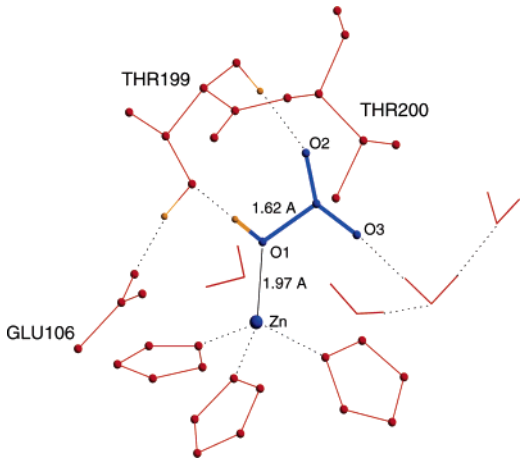

Figure 5. Minimum energy structure of zinc-bound bicarbonate and surrounding important residues (structure I). Dashed lines depict hydrogen bonds.

In both structures, the formed bond C−O1 is weak and elongated to 1.62 Å (structure II: 1.52 Å), as compared to a vacuum value of 1.43 Å. The corresponding bond order is 0.51 (structure II: 0.63), which is also indicative of a weak bond. The relative arrangement of bicarbonate in the active site is similar for both structures examined and characterized by hydrogen donation of the hydroxide−zinc ligand to the side chain of THR199, which participates, in turn, in a tight hydrogen bond to the carboxylate of GLU106 ("doorkeeper"). The carboxylate oxygen O2 hydrogen bonds with the peptide NH of THR199, and O3 takes part in the hydrogen bond network with active site waters. Figure 5 shows a schematic representation of minimized structure I (structure II is similar). Detailed geometrical data for both minima and the bound carbon dioxide intermediate mentioned above can be found in Table 2. The entire arrangement resembles the most commonly accepted proposals which are based on THR200HIS mutants and structures complexed with HSO_3^-. It is also in good

(74) Fierke, C. A.; Calderone, T. L.; Krebs, J. F. *Biochemistry* **1991**, *30*, 11054−11063.
(75) Alexander, R. S.; Nair, S. K.; Christianson, D. W. *Biochemistry* **1991**, *30*, 11064−11072.

Table 2. Geometrical Data for Bound Carbon Dioxide (Termed "Intermediate") and Both Optimized Structures for Bound Bicarbonate[a]

	distance [Å]			
system	Zn–O1	C–O1	C–O2	C–O3
intermediate	1.89	2.39	1.19	1.19
min I	1.97	1.62	1.23	1.25
min II	2.01	1.52	1.22	1.24

[a] Most notable is the elongated bond C−O1, as compared to a vacuum value of 1.43.[55] All values have been calculated employing hybrid density functional methods (B3LYP) with a 6-311++G(d,p) basis for the QM region.

coincidence with other quantum chemical studies. The main difference which arises when the arrangement is compared to the suggested structures[18] and to ab initio vacuum studies[61,62] is the elongated bond O1−C, which has, however, already been proposed by Garmer[61] by means of an effective interaction model. Single-point energies, obtained by using a 6-311++G-(d,p) basis set B3LYP/DFT method for the QM part of the QM/MM potential, have been calculated for the two optimized geometries of structures I and II and also for the bound carbon dioxide mentioned above. As a result, structure II has a relative energy of +6.89 kcal/mol as compared to bound carbon dioxide, whereas the energy of structure I is 13.71 kcal/mol lower than that of structure II. All minima have been verified by the calculation of numerical second derivatives. The high energy difference between structures I and II is most likely due to the strained bond. From these findings, structure I is best characterized as a high-energy intermediate which could stabilize − possibly induced by fluctuations in the backbone dihedral angle Ψ_{199} − to structure II or proceed in the catalytic cycle. Liljas et al. propose a weaker binding of bicarbonate to zinc from unfavorable interactions of the carboxylic part of bicarbonate with the hydrophobic cavity.[43] Indeed, the found arrangement of the carboxylate group results in an elongated bond in bicarbonate for both structures I and II and might thus contribute to the lowering of the binding affinity of bicarbonate. Atom charges and bond orders can be found in Table 1.

Dissociation of Bicarbonate. In the following discussion, the dissociation step of the bound bicarbonate has been studied. For the QM/MM setup, the inclusion of a water molecule into the QM zone was required. An appropriate candidate was the nearest water molecule to the zinc ion, which was 3.40 Å away. The closest water to the zinc ion in the original X-ray structure[16] which does not take part in the suggested proton relay mechanism is the "deep water" W338 (where the nomenclature introduced by Hakansson et al. was employed) with a distance of 4.04 Å. However, several water molecules have been displaced by the incoming substrate, and W265, at a distance of 5.60 Å away in the X-ray structure, is in the nearest position. Other water molecules might be equally suited to displace bicarbonate; however, the following studies focus on product dissociation when the water molecule has approached near to the zinc ion, and thus the choice of the "correct" replacement water is secondary.

In the first step, the water molecule was forced by constraints to a distance of 2.0 Å from the zinc ion. As the starting structure, the minimized geometry of structure I discussed above was used. After relaxation of the constraint and minimization, a pentacoordinated complex resulted with a (water-)oxygen to zinc

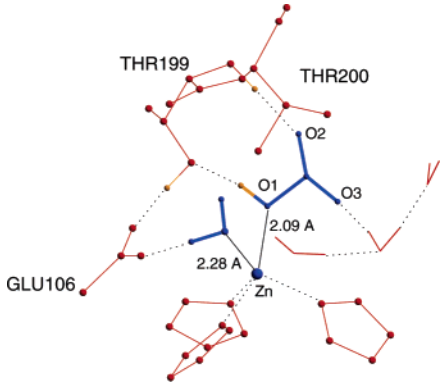

Figure 6. Minimum energy structure of a pentacoordinated intermediate in the process of dissociation of bicarbonate. The highlighted water molecule was additionally treated by QM methods in the QM/MM hybrid potential. The network of hydrogen bonds is drawn with dashed lines.

distance of 2.28 Å and a O1−Zn distance of 2.09 Å (Figure 6). The elongated bond O1−C is also shortened by 0.08 Å to 1.54 Å.

Several mechanisms have been proposed to account for the extraordinarily efficient catalysis of CO_2 hydration accomplished by HCA II, which requires a rapid dissociation of bicarbonate from the active site. The Lindskog and Lipscomb schemes[4,5,46] involve a rotation of bicarbonate or a hydrogen transfer to facilitate this. Studies of these reactions, which might contribute to a lowering of the dissociation barrier, are currently being undertaken. For an estimate of the required energy to dissociate bicarbonate, a potential energy scan was performed. The distance Zn−O1 was constrained to fixed values, and the energy was minimized for all other degrees of freedom. The resulting energies are shown in Figure 7. From these data, a barrier for dissociation of 6.2 kcal/mol has to be overcome. The minimized structure for the corresponding distance shows a broken hydrogen bond between the hydroxide oxygen of THR199 and the hydroxide of bicarbonate, but both oxygens involved are still at a close distance of 2.61 Å, which might result in a strong repulsive Pauli interaction. The other hydrogen bond observed, NH of THR199 to the O2 of bicarbonate, is still intact. As soon as the oxygen of bicarbonate exceeds a distance of 2.5 Å away from zinc, the water molecule is tightly coordinated at a distance of 2.0 Å.

Krebs et al.[30] find an increase in bicarbonate binding for a variant lacking the side-chain hydroxyl group of THR199. This is explained by a binding of bicarbonate when one of the negatively charged carboxylate oxygens binds to zinc, and thus, instead of a hydrogen bond to the hydroxide of THR199, a non-hydrogen bonded van der Waals contact is formed. Ab initio in vacuo calculations predict an almost barrierless dissociation[55] of bicarbonate. From these findings and the calculated energy barrier of 6.2 kcal/mol, which is relatively high, the occurrence of proton-transfer steps in the course of the catalytic cycle, leading to a destabilization of the bound bicarbonate, might be conjectured.

Summary and Conclusions

The process of bicarbonate formation catalyzed by HCA II has been studied with a QM/MM approach using the density functional theory as the QM method. The process of carbon dioxide hydration and bicarbonate dehydration was the main goal of this study. The influence of the protein environment is

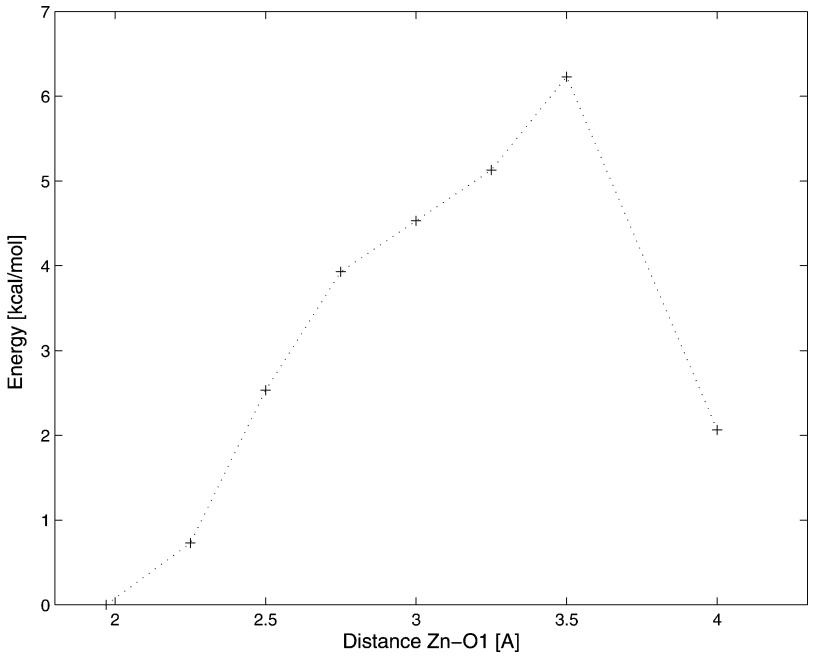

Figure 7. Potential energy as a function of the distance Zn−O1. This distance has been constrained to fixed values, and the energy has been optimized for all other degrees of freedom. An energy barrier of 6.2 kcal/mol is the maximum energy to be overcome in the scanned range. This occurs at a distance of 3.5 Å where the bond Zn−O1 is already broken and bicarbonate is formally dissociated.

taken into account by the nature of QM/MM methods and is shown to be significant here. Depending on the backbone angle Ψ_{199}, the hydration efficiency of carbon dioxide is considerably altered. In structures characterized by a backbone angle of $\Psi_{199} \approx 0°$, which can be found in most X-ray structures, a binding site for carbon dioxide is localized 2.48 Å away from the zinc-bound hydroxide. However, for dihedral angles of $\Psi_{199} \approx -34°$, the binding site is destroyed, and carbon dioxide diffuses directly to the zinc-bound hydroxide. This differing behavior is most likely due to short-range repulsive interactions of the substrate with the NH of THR200 which points in this arrangement toward the binding site. Possibly, a spectrum of binding modes of carbon dioxide extending between the two conformations described in this work exists. Additionally, the experimentally known binding site for cyanate has been calculated by means of QM/MM methods and found to be in good coincidence with experiment.

Apart from environmental effects, which are considered in the QM/MM methodology, the examination of bond forming and bond breaking processes in an enzyme as well as the study of electronic structure has also been made possible.

As a consequence of the interaction of bound carbon dioxide with THR199, a significantly enhanced electrophilicity of the carbon, and thus facilitated product, formation results. The subsequently formed bicarbonate is similar to suggested and experimentally observed structures, characterized by hydrogen bonds to the side-chain oxygen and the peptide NH of THR199. The most remarkable feature of the found minimum energy structures is the occurrence of a weak elongated bond between the carbon of carbon dioxide and the oxygen of zinc-bound hydroxide. This, together with a destabilization of the carboxy part of bicarbonate in the hydrophobic binding site, might contribute to a better dissociation of bicarbonate.

The dissociation step was examined by inclusion of an additional water molecule to the QM region. A pentacoordinated intermediate was found, and a first estimate of the energy required for dissociation of bicarbonate is given. The found energy barrier is 6.2 kcal/mol. Part of the strain energy of the elongated bond C−O, which is already relaxed at this point, may have been realized in a lowering of this barrier. However, from a comparison with ab initio quantum chemical calculations and experimental data, an even lower barrier may be expected.

Acknowledgment. This work was supported by a grant of the Austrian Science Fund (grant number P13845-TPH).

JA035072F